Title

Amyloid β-sheet mimics that antagonize protein aggregation and reduce amyloid toxicity.

Permalink

https://escholarship.org/uc/item/4sn8246h

Journal

Nature chemistry, 4(11)

ISSN

1755-4330

Authors

Cheng, Pin-Nan
Liu, Cong
Zhao, Minglei
et al.

Publication Date

2012-11-01

DOI

10.1038/nchem.1433

Peer reviewed

Amyloid β-Sheet Mimics that Antagonize Amyloid Aggregation and Reduce Amyloid Toxicity

Pin-Nan Cheng[a], **Cong Liu**[b], **Minglei Zhao**[b], **David Eisenberg**[b], and **James S. Nowick**[a]

[a]Department of Chemistry, University of California, Irvine, Irvine, California CA 92697-2025

[b]UCLA-DOE Institute for Genomics and Proteomics, Howard Hughes Medical Institute, Molecular Biology Institute, University of California, Los Angeles, Los Angeles, California, CA 90095-1570

Abstract

The amyloid protein aggregation associated with diseases such as Alzheimer's, Parkinson's, and type II diabetes (among many others), features a bewildering variety of β-sheet-rich structures in transition from native proteins to ordered oligomers and fibers. The variation in the amino acid sequences of the β-structures presents a challenge to developing a model system of β-sheets for the study of various amyloid aggregates. Here we introduce a family of robust β-sheet macrocycles that can serve as a platform to display a variety of heptapeptide sequences from different amyloid proteins. We have tailored these amyloid β-sheet mimics (ABSMs) to antagonize aggregation of various amyloid proteins, thereby reducing the toxicity of amyloid aggregates. We describe the structures and inhibitory properties of ABSMs containing amyloidogenic peptides from Aβ associated with Alzheimer's disease, β_2-microglobulin associated with dialysis-related amyloidosis, α-synuclein associated with Parkinson's disease, islet amyloid polypeptide associated with type II diabetes, human and yeast prion proteins, and Tau, which forms neurofibrillary tangles.

Introduction

Amyloid aggregation is associated with many intractable protein aggregation diseases, notably including Alzheimer's disease, Huntington's disease, Parkinson's disease, type II diabetes, and prion diseases[1–3]. Amyloid fibrils with characteristic highly ordered cross-β structures are the ultimate products of amyloid aggregation. More than 30 proteins have been linked to amyloidogenesis and they exhibit enormous variations in sequences and polymorphic fibril structures[1,4–6]. Fibril formation of a given polypeptide, however, greatly

Corresponding Authors: James S. Nowick, jsnowick@uci.edu, 949-824-6091, Department of Chemistry, University of California, Irvine, CA 92697-2025. David Eisenberg, david@mbi.ucla.edu, 310-825-3754, Department of Chemistry and Biochemistry, University of California, Los Angeles, 611 Charles Young Dr. East, Los Angeles, CA 90095-1569.
[1]P.-N.C. and C.L. contributed equally to this work.

depends on its specific residue order[7,8]. Crystallographic structures of amyloidlike fibrils formed by amyloidogenic peptide fragments suggest that the formation of highly-ordered parallel or antiparallel β-sheets and a steric-zipper interface between β-sheets are two essential elements for amyloid fibril formation[9,10].

While amyloid fibrils are the most visible evidence of pathology, soluble oligomers are proving to be more important in amyloid toxicity[11,12]. Although increasing evidence shows that these transient, unstable structures are rich in β-sheets, their dynamic and polymorphic properties make amyloid oligomers difficult to study at the atomic level[13–15]. Additional tools are needed to study amyloid oligomers and aggregation and to shed light on controlling these processes.

β-Sheet mimics that can display amyloid β-strands provide a means to study amyloid oligomers and aggregation. We previously introduced 42-membered ring macrocyclic β-sheets containing pentapeptide fragments from amyloid-β peptide (Aβ) and tau protein (Tau) to mimic amyloidlike β-sheets and shed a light on the structures of transient amyloid oligomers[16,17]. We have also used these macrocyclic β-sheets to inhibit aggregation of the peptide Ac-VQIVYK-NH$_2$ (AcPHF6) derived from Tau to provide insights into the aggregation process[18].

The development of a robust chemical model of β-sheets that can tolerate a variety of amino acid sequences has been challenging because amyloidogenic sequences vary enormously and because folding of β-sheet mimics largely depends on the amino acid sequence[1,19]. In this paper, we introduce a new class of β-sheet macrocycles that can tolerate a wide range of amino acid sequences from amyloid proteins and still fold into β-sheet structures. We call these macrocycles amyloid β-sheet mimics (ABSMs).

ABSM **1** is a 54-membered ring and comprises a heptapeptide β-strand (the upper strand), one Hao unit flanked by two dipeptides (the lower strand), and two δ-linked ornithine ($^\delta$Orn) turns (Figure 1a). The "upper" β-strand of ABSM **1** incorporates different heptapeptide fragments from Aβ, Tau, yeast Sup35 prion protein (Sup35), human prion protein (hPrP), human β$_2$-microglobulin (hβ$_2$M), human α-synuclein (hαSyn), and human islet amyloid polypeptide (hIAPP). Hao is a tripeptide β-strand mimic that not only serves as a template for *intra*molecular hydrogen bonding but also minimizes the exposed hydrogen-bonding functionality of the "lower" strand[20]. This structural design of Hao helps prevent ABSMs **1** from aggregating in solution to form an infinite network of in-register β-sheets; instead, ABSMs **1** dimerize and then further self-assemble into oligomers. The "upper" and "lower" strands of ABSM **1** are connected by two $^\delta$Orn β-turn mimics[21].

We envisioned that ABSM **1** would fold well because it is conformationally constrained by cyclicity and has a Hao template to promote *intra*molecular hydrogen bonding and two $^\delta$Orn β-turn mimics to promote turn formation. We also envisioned that four pairs of side chains (R$_1$–R$_{11}$, R$_2$–R$_{10}$, R$_6$–R$_9$, and R$_7$–R$_8$) would provide stabilizing transannular interactions. We anticipated that the flexibility of the dipeptides flanking Hao in the "lower" strand would better accommodate the flatness of the Hao template and thus minimize the kinks in the β-strands that we had previously observed in the 42-membered ring macrocycles[17].

We designed ABSMs **1** to display exposed heptapeptide β-strands so that these β-strands can recognize and bind their parent amyloid proteins (Figure 1b). We envisioned recognition between ABSMs **1** and their parent amyloid proteins to take place through the β-sheet interactions observed in amyloid aggregation.

Here, we present structural studies of these ABSMs **1** and describe their effect upon amyloid aggregation and toxicity.

Results

1. Design of Amyloid β-Sheet Mimics 1

To test the folding of ABSMs **1**, we selected 16 amyloidogenic heptapeptide β-strands from seven β-sheet-rich amyloid proteins for positions 1–7 in the "upper" strands (Table 1). ABSMs **1a–g** contain heptapeptide sequences from two important hydrophobic and fibril-forming regions of Aβ associated with Alzheimer's disease, residues 16–23 and 29–40[5, 22]. ABSMs **1a–d** and **f** contain native heptapeptide sequences, while ABSMs **1e** and **1g** are G33F and G37F mutants, in which the aromatic residue across from Hao promotes better folding[16]. ABSM **1h** contains residues 7–13 from Sup35, which has been widely used as a model to study amyloid formation[9]. ABSM **1i** contains residues 116–122 from hPrP, which is the infectious agent of prion diseases[23]. ABSM **1j** contains residues 305–311 from Tau, which forms neurofibrillary tangles[24]. ABSM **1k–m** contain residues 62–68 and 63–69 from hβ$_2$M associated with dialysis-related amyloidosis[25]. ABSMs **1n** and **1o** contain residues 69–75 and 75–81 from hαSyn associated with Parkinson's disease[26]. ABSMs **1p** and **1q** contain residues 11–17 and 26–32 from hIAPP associated with type II diabetes[27]. We chose polar and hydrophobic residues at positions 8–11 in the "lower" strands of ABSMs **1** to promote solubility in water and to increase hydrophobic residues that favor β-sheet formation.

2. Synthesis of Amyloid β-Sheet Mimics 1

ABSMs **1** were prepared by synthesizing the corresponding protected linear peptides, followed by solution-phase cyclization and deprotection[28]. The protected linear peptide precursors were synthesized on 2-chlorotrityl chloride resin by conventional Fmoc-based solid-phase peptide synthesis. Macrocyclization was typically performed using HCTU and *N,N*-diisopropylethylamine in DMF at ca. 0.5 mM concentration. The ABSMs **1** were isolated in ca. 20–30% overall yield after HPLC purification and lyophilization. Each synthesis produces tens of milligrams of ABSMs **1** as fluffy white solids. (For details, see the Supplementary Information Text.)

3. X-Ray Crystallographic Studies of Amyloid β-Sheet Mimic 1r

X-ray crystallography of ABSM **1r** validates the design of ABSMs **1** (Figure 2). ABSM **1r** is a homologue of ABSM **1d** in which the Tyr residue in the "lower" strand is replaced with 4-bromophenylalanine for crystallographic phase determination. ABSM **1r** adopts a β-sheet structure in which the "upper" and "lower" strands are *intra*molecularly hydrogen-bonded to form eight hydrogen bonds (Figure 2a). The two [8]Orn residues of ABSM **1r** fold into β-turn

like conformations, Hao mimics a tripeptide β-strand, and the "upper" strand displays an exposed heptapeptide β-sheet edge.

ABSM **1r** forms a dimer in the crystal lattice in which the two recognition β-strands come together in an antiparallel β-sheet fashion (Figure 2b). The β-strands of the dimerization interface are shifted out of register, forming only six hydrogen bonds instead of the eight that would form through in-register contact.

The dimers stack in the crystal lattice, with hydrophobic contacts between the layers of the stack. The Ile, Leu, and Val, at positions 3, 5, and 7 on the "top" face of the dimer pack together in one set of hydrophobic contacts "above" the dimer, while the Met and Phe at positions 6 and 9 on the "bottom" face of the dimer pack together in another set of hydrophobic contacts "below" the dimer (Figures 2c and 2d). The hydrophobic contacts between the dimer layers appear to be important in the crystallization and supramolecular assembly of ABSM **1r** and may explain the formation of the out-of-register interface within the dimer.

4. ^{1}H NMR Studies of Amyloid β-Sheet Mimics 1

^{1}H NMR studies of ABSMs **1a–q** in D_2O solution further validate the design of ABSMs **1** and establish that ABSMs **1** generally adopt folded β-sheet structures in solution. The ^{1}H NMR spectra of ABSMs **1** show sharp, disperse resonances at submillimolar and low millimolar concentrations in D_2O solution, suggesting ABSMs **1** to be non-aggregating in water. Antiparallel β-sheets have close contacts between the α-protons of the non-hydrogen-bonded pairs of amino acids, which generally give strong *inter*strand NOE cross-peaks (NOEs). In ABSMs **1**, these close contacts should involve the α-protons of residues 2 and 10 (2–10) and residues 6 and 9 (6–9). There should also be homologous contacts involving the α-proton of residue 4 and H_6 of Hao (4-Hao$_6$) and the α- and *pro-S* δ-protons of the $^\delta$Orn turns (Orn$_{\alpha-\delta S}$). Table 1 illustrates these contacts.

All ABSMs, except **1h**, **1i**, and **1l**, exhibit most of these key NOEs (Table 1). ABSMs **1a–e**, **1g**, **1j**, **1k**, and **1m–q** show strong 2–10, 6–9, 4-Hao$_6$, and Orn$_{\alpha-\delta S}$ NOEs and thus exhibit good folding. ABSM **1f** shows strong Orn$_{\alpha-\delta S}$ and 2–10 NOEs and a weak 4-Hao$_6$ NOE and thus exhibits moderate folding. ABSMs **1h**, **1i**, and **1l** show only Orn$_{\alpha-\delta S}$ NOEs and thus exhibit weak folding. Although the lack of the *inter*strand NOEs indicates poor folding of ABSMs **1h**, **1i**, and **1l**, the Orn$_{\alpha-\delta S}$ NOEs suggest that their $^\delta$Orn residues fold at least partially into a β-turn like conformation. Table 1 summarizes the observed key NOEs and the folding of ABSMs **1**.

5. Inhibition of Amyloid Aggregation by Amyloid β-Sheet Mimics 1

Thioflavin T (ThT) fluorescence assays and transmission electron microscopy (TEM) studies show that the ABSMs containing amyloidogenic sequences can inhibit aggregation of amyloid proteins. We studied inhibition of Aβ$_{40}$ and Aβ$_{42}$ aggregation by ABSM **1a**, inhibition of hβ$_2$M aggregation by ABSM **1m**, and inhibition of truncated human α-synuclein (hαSyn$_{1–100}$) aggregation by ABSM **1o**.

ThT fluorescence assays show that ABSMs **1a**, **1m**, and **1o** effectively delay aggregation of their parent proteins at sub-stoichiometric concentrations in a dose-dependent manner (Figures 3a–d). ABSM **1a** delays $A\beta_{40}$ and $A\beta_{42}$ aggregation by 280% and 350% respectively at 0.2 equivalents and by 430% and 600% at 0.5 equivalents (Figures 3a and 3b). Although ThT fluorescence assays show that $A\beta$ aggregation exhibits comparable lag times at 0.5 and 1.0 equivalents of ABSM **1a**, the growth phases of the aggregation are much slower at 1.0 equivalent than at 0.5 equivalents. (* in Figures 3a and 3b. For details, see Figures S1 and S2.) ABSM **1m** delays $h\beta_2M$ aggregation by 160% at 0.2 and 0.5 equivalents and by 340% at 1.0 equivalent (Figure 3c). ABSM **1o** delays $h\alpha Syn_{1-100}$ aggregation by 150% at 0.2 equivalents (Figure 3d). Although $h\alpha Syn_{1-100}$ aggregation exhibits longer lag times with 0.5 and 1.0 equivalents of ABSM **1o** than with 0.2 equivalents, some runs showed complete suppression of aggregation, while other runs showed typical sigmoidal curves. Because of this scatter in the data, the precise lag times are not reported. (* in Figure 3d. For details, see Figure S4.) TEM studies of samples taken directly from the ThT assays show that $A\beta$, $h\beta_2M$, and $h\alpha Syn_{1-100}$ form fibrils without ABSMs and do not form fibrils with ABSMs (1.0 equivalent) during the delayed lag time (Figures 3eh).

$A\beta$ has been shown to cross-interact with different amyloidogenic proteins containing similar primary sequences[29–31]. To investigate cross-interaction of $A\beta$ with ABSMs, we compared the interaction of $A\beta$ with ABSM **1a** to that with ABSM **1m**, which has a closely homologous sequence, and to that with ABSM **1o**, which does not (Figure S5). ThT fluorescence assays show that ABSM **1m** inhibits $A\beta$ aggregation, like ABSM **1a**, while ABSM **1o** has little or no inhibitory effect (Figure S5). This result suggests that structurally homologous ABSMs can not only interact with their parent amyloid proteins but can also cross interact with different amyloid proteins.

To further investigate the effect of sequence on inhibition, we compared the interaction of ABSM **1a** with $A\beta_{40}$ to that of ABSMs 1b, **1c**, **1d**, and **1f** with $A\beta_{40}$. ThT fluorescence assays show that ABSM **1b** is effective against $A\beta_{40}$ aggregation, while ABSMs **1c**, **1d**, and **1f** cause little or no inhibition (Figure S6). The inhibition of $A\beta_{40}$ aggregation by both ABSMs **1a** and **1b** indicates that the central hydrophobic sequence $A\beta_{17-21}$ is critical to the activity of ABSMs against $A\beta_{40}$ aggregation. This result supports the role of $A\beta_{17-21}$ in $A\beta$ aggregation and suggests that strong interaction of this sequence in these ABSMs with that of the $A\beta$ oligomers delays $A\beta$ aggregation[22, 32].

6. Detoxification of Aβ by Amyloid β-Sheet Mimic 1a

Cell viability (MTT) assays establish that ABSM **1a** reduces the toxicity of $A\beta_{40}$ and $A\beta_{42}$ in PC-12 cells (Figure 4) and that ABSMs **1a**, **1m**, and **1o** exhibit little or no toxicity (Figure S9). We examined the effect of ABSM **1a** on the toxicity of $A\beta_{40}$ and $A\beta_{42}$, because ABSM **1a** exhibits the best inhibitory activity among those studied. We first incubated $A\beta$ monomers (5μM) without ABSM **1a** to allow $A\beta$ oligomers and fibrils to form. The resulting $A\beta$ mixtures were directly used in cell viability assays. These assays show that the $A\beta_{40}$ and $A\beta_{42}$ preincubated without ABSM **1a** kills 42% and 46% of the PC-12 cells

respectively, relative to controls in which the cells are incubated in only PBS buffer solutions (Figure 4).

Cell viability assays further establish that preincubation of Aβ with ABSM **1a** rescues the cells in a dose-dependent manner. Preincubation of Aβ$_{40}$ and Aβ$_{42}$ with 0.2 equivalents of ABSM **1a** reduces the death of PC-12 to 29% and 38% respectively, while preincubation with 1.0 equivalent reduces cell death to 27% and 30% and preincubation with 5 equivalents reduces cell death to 14% and 6%. The rescue of these neuron like cells by ABSM **1a** suggests that ABSMs may reduce the production of toxic amyloid oligomers or bind the oligomers and reduce their toxicity.

Discussion

Amyloid β-sheet mimics **1** provide a unique tool with which to elucidate the process of amyloid aggregation. Although many of the details of amyloid aggregation still remain unclear, nucleation-dependent polymerization, in which seeding to form a β-structured nucleus is the rate-determining step, is widely accepted[1, 22]. Based on the nucleation-dependent polymerization, we propose a model for the potent inhibition of Aβ aggregation by ABSM **1a**. In this model, ABSM **1a** binds early β-structured oligomers and blocks Aβ nucleation (Figure 5a). Without ABSM **1a**, the unstructured monomer forms β-structured oligomers which, in the rate-determining step, go on to form a β-structured nucleus that ultimately assembles to form cross-β fibrils. The solid line in Figure 5a illustrates this pathway. ABSM **1a** creates a new aggregation pathway for the early β-structured oligomers. In this pathway, ABSM **1a** binds the β-structured oligomers to form Aβ-oligomer-ABSM-**1a** complexes and blocks the Aβ oligomer-to-nucleus transition. The dashed line in Figure 5a illustrates this pathway.

It is significant that ABSM **1a** substantially delays the aggregation of Aβ at sub-stoichiometric concentrations (as low as 1 μM), e.g. 0.05 equivalents of ABSM **1a** per equivalent of Aβ (Figure S2), while simple linear peptide fragments derived from Aβ generally show substantial inhibitory effects at stoichiometric or greater concentrations[33,34]. This observation suggests that ABSM **1a** binds a larger oligomer, not the monomer or a smaller oligomer, such as a dimer, trimer, or tetramer. ABSM **1a** binds the early β-structured oligomers more strongly than the unstructured monomers bind oligomers, because the recognition β-strand of ABSM **1a** is preorganized. This preorganization thus promotes formation of Aβ-oligomer-ABSM-**1a** complexes. The complexation may occur through edge-to-edge interactions between the hydrogen-bonding edge of ABSM **1a** and exposed hydrogen-bonding groups of the Aβ oligomers and through face-to-face hydrophobic interactions between ABSM **1a** and the hydrophobic surfaces of the Aβ oligomers. These types of interactions should take place between the hydrophobic sequence Aβ$_{17-21}$ of ABSM **1a** and that of the Aβ oligomers, as observed in the amyloid-related oligomers containing the pentapeptide sequence LVFFA shown in Figure 5b and the amyloidlike fibrils from the hexapeptide KLVFFA shown in Figure 5c. Similar interactions should also occur in the interactions of other ABSMs with their parent amyloidogenic peptides and proteins. The stabilization of these complexes creates a higher energy barrier to formation of the β-structured nucleus and thus delays or halts fibril formation. Because ABSM **1a** cannot

sequester all of the equilibrating Aβ oligomers, the Aβ monomers and oligomers eventually succumb to thermodynamics and form Aβ fibrils.

The X-ray crystallographic structure of ABSM **1r** may provide insights not only into the stabilization of the dimerization and higher-order supramolecular assembly of ABSMs, but also into the stabilization and structure of intermediates formed during amyloid aggregation. The hydrophobic contacts formed by the Ile, Leu, and Val, at positions 3, 5, and 7 of ABSM **1r** are akin to the steric zipper of amyloidlike fibrils formed by fragments $A\beta_{16-21}$, $A\beta_{30-35}$, $A\beta_{35-40}$, and $A\beta_{37-42}$[10, 35]. Both the layered crystal structure of ABSM **1r** and the amyloidlike fibrils are stabilized by hydrophobic contacts. These observations suggest that maximization of both hydrophobic contact and hydrogen bonding is key to stabilizing not only amyloid fibrils but also transient amyloid oligomers[36].

Conclusion

The amyloid β-sheet mimics **1** described herein provide a single platform with which to display a variety of amyloidogenic heptapeptide β-strands and provide a rational design for inhibitors to control amyloid aggregation. X-ray crystallographic and ^{1}H NMR studies validate that the design of ABSMs **1**, including the cyclicity, Hao template, two $^{\delta}$Orn β-turn mimics, and paired side chains, promotes the formation of β-sheets in which the folding is largely independent of the amino acid sequence.

ABSMs **1** can be tailored to inhibit aggregation of different amyloid proteins. The inhibition of Aβ, $h\beta_2M$, and $h\alpha Syn_{1-100}$ aggregation by ABSMs **1** indicates that ABSMs containing one hydrogen-bonding edge and one blocking edge are an effective design for inhibitors of amyloid aggregation. The ability of ABSMs **1a**, **1m**, and **1o** to inhibit amyloid aggregation and to detoxify amyloid aggregates suggests the potential for therapeutic applications in amyloid-related diseases.

Materials and Methods

Synthetic $A\beta_{40}$ was purchased from GL Biochem (Shanghai) Ltd. $A\beta_{42}$, $h\beta_2M$, and $h\alpha Syn_{1-100}$ were expressed in *E. coli.* (For details, see the Supplementary Information Text.) ABSMs **1** were synthesized as described above. (For details, see the Supplementary Information Text.) ^{1}H NMR, 2D TOCSY, and 2D ROESY experiments of ABSMs **1** were performed in D_2O with DSA as an internal standard at 500 MHz at 298 K. (For details, see the Supplementary Information Text.) Crystallization, data collection, and structure determination of ABSM **1r** are described in the Supplementary Information Text. ThT fluorescence assays and TEM studies of Aβ, $h\beta_2M$, and $h\alpha Syn_{1-100}$ aggregation with ABSMs **1a**, **1m**, and **1o** are described in the Supplementary Information Text. Cell viability assays to establish the toxicity of ABSMs **1a**, **1m**, and **1o** toward HeLa, HEK-293, and PC-12 cells are described in the Supplementary Information Text.

Supplementary Material

Refer to Web version on PubMed Central for supplementary material.

Acknowledgments

References

1. Chiti F, Dobson CM. Protein misfolding, functional amyloid, and human disease. Annu Rev Biochem. 2006; 75:333–366. [PubMed: 16756495]

2. Aguzzi A, O'Connor T. Protein aggregation diseases: pathogenicity and therapeutic perspectives. Nat Rev Drug Discov. 2010; 9:237–248. [PubMed: 20190788]

3. Bartolini M, Andrisano V. Strategies for the inhibition of protein aggregation in human diseases. ChemBioChem. 2010; 11:1018–1035. [PubMed: 20401887]

4. Greenwald J, Riek R. Biology of amyloid: structure, function, and regulation. Structure. 2010; 18:1244–1260. [PubMed: 20947013]

5. Tycko R. Solid-state NMR studies of amyloid fibril structure. Annu Rev Phys Chem. 2011; 62:279–299. [PubMed: 21219138]

6. Eichner T, Radford SE. A diversity of assembly mechanisms of a generic amyloid fold. Mol Cell. 2011; 43:8–18. [PubMed: 21726806]

7. Lopez de la Paz M, Serrano L. Sequence determinants of amyloid fibril formation. Proc Natl Acad Sci USA. 2004; 101:87–92. [PubMed: 14691246]

8. Goldschmidt L, Teng PK, Riek R, Eisenberg D. Identifying the amylome, proteins capable of forming amyloid-like fibrils. Proc Natl Acad Sci USA. 2010; 107:3487–3492. [PubMed: 20133726]

9. Nelson R, et al. Structure of the cross-β spine of amyloid-like fibrils. Nature. 2005; 435:773–778. [PubMed: 15944695]

10. Sawaya MR, et al. Atomic structures of amyloid cross-β spines reveal varied steric zippers. Nature. 2007; 447:453–457. [PubMed: 17468747]

11. Conway KA, et al. Acceleration of oligomerization, not fibrillization, is a shared property of both α-synuclein mutations linked to early-onset Parkinson's disease: Implications for pathogenesis and therapy. Proc Natl Acad Sci USA. 2000; 97:571–576. [PubMed: 10639120]

12. Lashuel HA, Hartley D, Petre BM, Walz T, Lansbury PT. Neurodegenerative disease: Amyloid pores from pathogenic mutations. Nature. 2002; 418:291–291. [PubMed: 12124613]

13. Chimon S, et al. Evidence of fibril-like β-sheet structures in a neurotoxic amyloid intermediate of Alzheimer's β-amyloid. Nat Struct Mol Biol. 2007; 14:1157–1164. [PubMed: 18059284]

14. Bernstein SL, et al. Amyloid-β protein oligomerization and the importance of tetramers and dodecamers in the aetiology of Alzheimer's disease. Nat Chem. 2009; 1:326–331. [PubMed: 20703363]

15. Ono K, Condron MM, Teplow DB. Structure–neurotoxicity relationships of amyloid β-protein oligomers. Proc Natl Acad Sci USA. 2009; 106:14745–14750. [PubMed: 19706468]

16. Woods RJ, et al. Cyclic modular β-sheets. J Am Chem Soc. 2007; 129:2548–2558. [PubMed: 17295482]

17. Liu C, et al. Characteristics of amyloid-related oligomers revealed by crystal structures of macrocyclic β-sheet mimics. J Am Chem Soc. 2011; 133:6736–6744. [PubMed: 21473620]

18. Zheng J, et al. Macrocyclic β-sheet peptides that inhibit the aggregation of a tau-protein-derived hexapeptide. J Am Chem Soc. 2011; 133:3144–3157. [PubMed: 21319744]

19. Gellman SH. Minimal model systems for β-sheet secondary structure in proteins. Curr Opin Chem Biol. 1998; 2:717–725. [PubMed: 9914187]

20. Nowick JS, et al. An unnatural amino acid that mimics a tripeptide β-strand and forms β-sheet like hydrogen-bonded dimers. J Am Chem Soc. 2000; 122:7654–7661.

21. Nowick JS, Brower JO. A new turn structure for the formation of β-hairpins in peptides. J Am Chem Soc. 2003; 125:876–877. [PubMed: 12537479]

22. Finder VH, Glockshuber R. Amyloid-β aggregation. Neurodegener Dis. 2007; 4:13–27. [PubMed: 17429215]

23. Walsh P, Simonetti K, Sharpe S. Core structure of amyloid fibrils formed by residues 106 126 of the human prion protein. Structure. 2009; 17:417–426. [PubMed: 19278656]

24. Friedhoff P, von Bergen M, Mandelkow EM, Davies P, Mandelkow E. A nucleated assembly mechanism of Alzheimer paired helical filaments. Proc Natl Acad Sci USA. 1998; 95:15712–15717. [PubMed: 9861035]

25. Platt GW, Routledge KE, Homans SW, Radford SE. Fibril growth kinetics reveal a region of β_2-microglobulin important for nucleation and elongation of aggregation. J Mol Biol. 2008; 378:251–263. [PubMed: 18342332]

26. Vilar M, et al. The fold of α-synuclein fibrils. Proc Natl Acad Sci USA. 2008; 105:8637–8642. [PubMed: 18550842]

27. Luca S, Yau WM, Leapman R, Tycko R. Peptide conformation and supramolecular organization in amylin fibrils: Constraints from Solid-State NMR. Biochem. 2007; 46:13505–13522. [PubMed: 17979302]

28. Cheng PN, Nowick JS. Giant macrolactams based on β-sheet peptides. J Org Chem. 2011; 76:3166–3173. [PubMed: 21452877]

29. Yan LM, Velkova A, Tatarek-Nossol M, Andreetto E, Kapurniotu A. IAPP mimic blocks Aβ cytotoxic self-assembly: cross-suppression of amyloid toxicity of Aβ and IAPP suggests a molecular link between Alzheimer's disease and Type II diabetes. Angew Chem, Int Ed. 2007; 46:1246–1252.

30. Seeliger J, et al. Cross-amyloid interaction of Aβ and IAPP at lipid membranes. Angew Chem, Int Ed. 2012; 51:679–683.

31. Ma B, Nussinov R. Selective molecular recognition in amyloid growth and transmission and cross-species barriers. J Mol Biol. 10.1016/j.jmb.2011.11.023

32. Miller Y, Ma B, Nussinov R. Polymorphism in Alzheimer Aβ amyloid organization reflects conformational selection in a rugged energy landscape. Chem Rev. 2010; 110:4820–4838. [PubMed: 20402519]

33. Stains CI, Mondal K, Ghosh I. Molecules that Target beta-Amyloid. ChemMedChem. 2007; 2:1674–1692. [PubMed: 17952881]

34. Sciarretta KL, Gordon DJ, Meredith SC. Peptide-based inhibitors of amyloid assembly. Methods Enzymol. 2006; 413:273–312. [PubMed: 17046402]

35. Colletier JP, et al. Molecular basis for amyloid-β polymorphism. Proc Natl Acad Sci USA. 2011; 108:16938–16943. [PubMed: 21949245]

36. Laganowsky A, et al. Atomic view of a toxic amyloid small oligomer. Science. 2012; 335:1228–1231. [PubMed: 22403391]
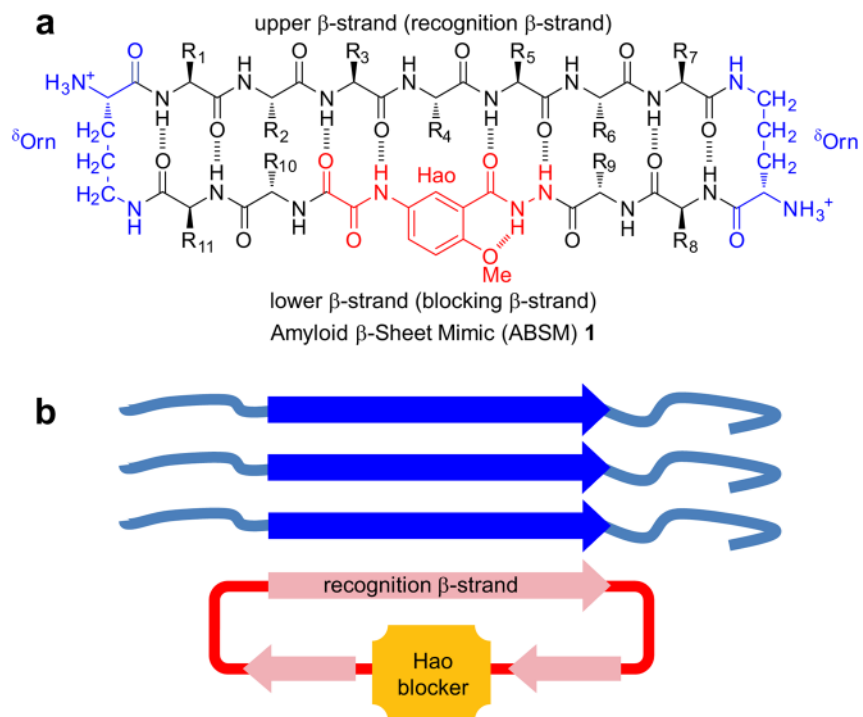
Figure 1.
Design of amyloid β-sheet mimic **1**. (a) Representation of ABSM **1** illustrating the upper β-strand (recognition β-strand), the δ-linked ornithine ($^{\delta}$Orn) turn unit, and the Hao amino acid blocker unit. (b) Representation of ABSM **1** recognizing and blocking amyloid aggregation through β-sheet interactions.
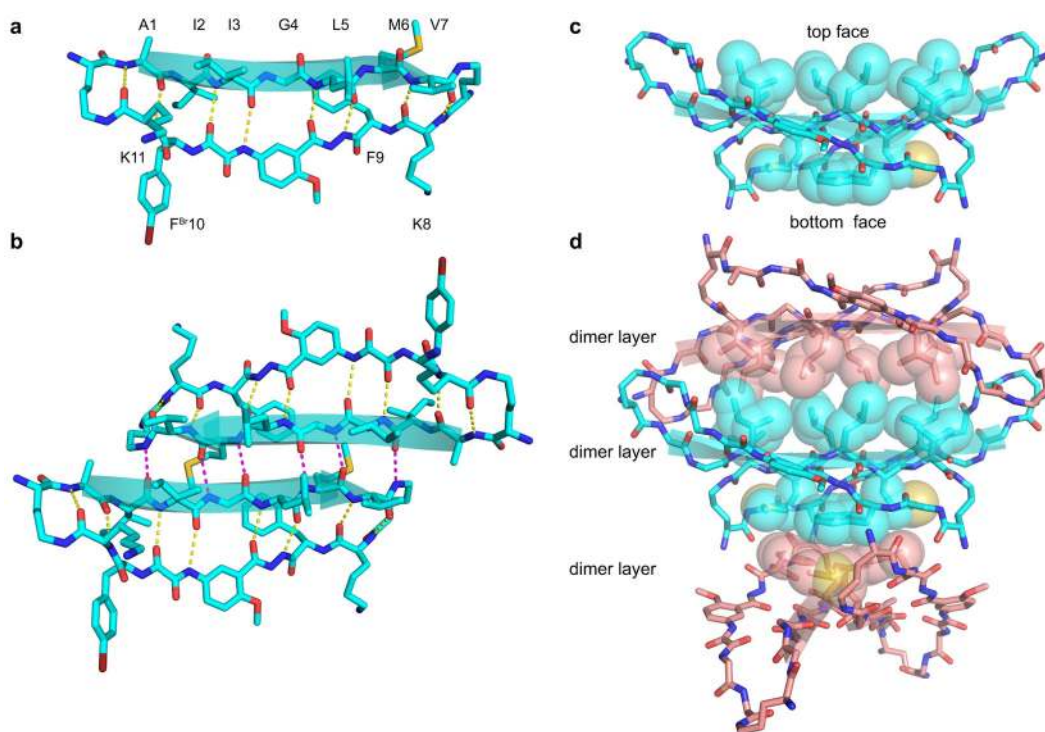
Figure 2.
X-ray crystallographic structure of ABSM **1r**, which contains the heptapeptide sequence
AIIGLMV (Aβ$_{30-36}$). (a) The monomer. (b) The dimer: top view. (c) The dimer: side view.
(d) Stacked layers of dimer in the crystal lattice. Note that the view in b is perpendicular to
the β-sheet (top view), whereas the view in c and d is 90° away, parallel to the β-sheet (side
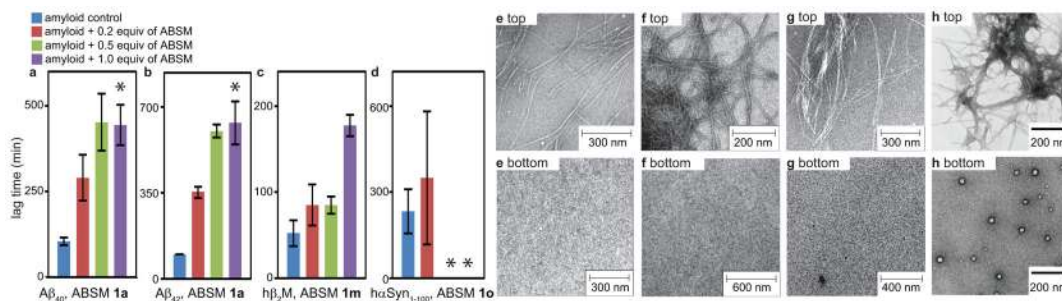view) and shows the hydrophobic contacts. Some side chains in c and d have been omitted
for clarity.

Figure 3.
Effect of ABSMs on inhibition of $A\beta_{40}$, $A\beta_{42}$, $h\beta_2M$, and $h\alpha Syn_{1-100}$ aggregation monitored by thioflavin T fluorescence assays and transmission electron microscopy. (a) Lag time of $A\beta_{40}$ (20 μM) aggregation in the absence and presence of ABSM **1a**. (b) Lag time of $A\beta_{42}$ (20 μM) aggregation in the absence and presence of ABSM **1a**. (c) Lag time of $h\beta_2M$ (30μM) aggregation in the absence and presence of ABSM **1m**. (d) Lag time of $h\alpha Syn_{1-100}$ (50μM) aggregation in the absence and presence of ABSM **1o**. (e) TEM of $A\beta_{40}$ (20 μM) after incubation for 6 h without ABSM **1a** (top) and incubation for 6 h with 1.0 equivalent of ABSM **1a** (bottom). (f) TEM of $A\beta_{42}$ (20 μM) after incubation for 7 h without ABSM **1a** (top) and incubation for 7 h with 1.0 equivalent of ABSM **1a** (bottom). (g) TEM of $h\beta_2M$ (30 μM) after incubation for 2 h without ABSM **1m** (top) and incubation for 2 h with 1.0 equivalent of ABSM **1m** (bottom). (h) TEM of $h\alpha Syn_{1-100}$ (50 μM) after incubation for 72 h without ABSM **1o** (top) and incubation for 72 h with 1.0 equivalent of ABSM **1o** (bottom). * For explanation, see the text and Figures S1, S2, and S4. Error bars correspond to standard deviation of four or greater sets of experiments. For experimental details, see the Supplementary Information Text.
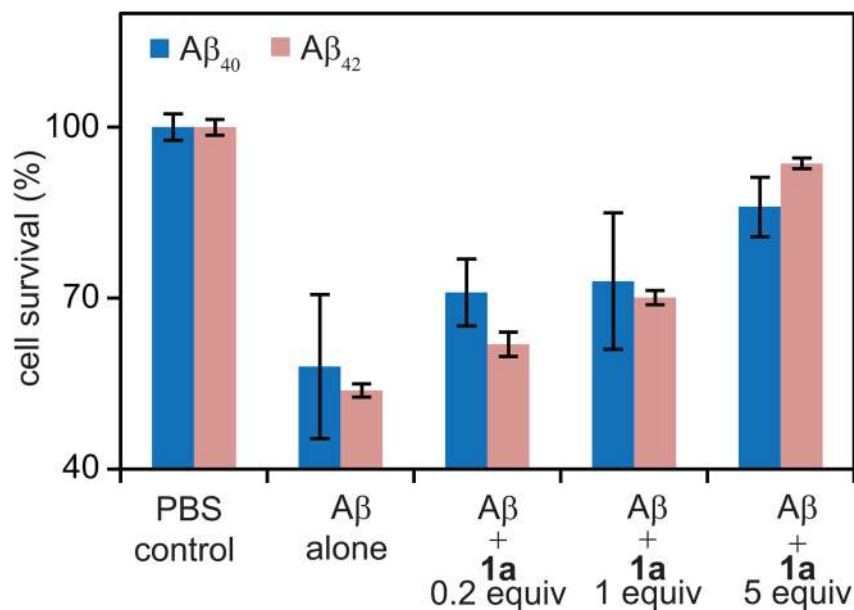
Figure 4.
Effect of ABSM **1a** on $A\beta_{40}$ and $A\beta_{42}$ toxicity toward PC-12 cells. Addition of $A\beta$ decreases cell survival when PC-12 cells are cultured for 24 h with preincubated $A\beta$. Cell survival increases when cells are cultured for 24 h with a preincubated mixture of ABSM **1a** and $A\beta$ in 0.2, 1.0, and 5 molar ratios. Cell survival is given as a percentage relative to controls in which only phosphate-buffered saline (PBS) is added. The cell survival of the PBS controls is taken to be 100%. Error bars correspond to standard deviation of four sets of experiments. For experimental details, see the Supplementary Information Text.
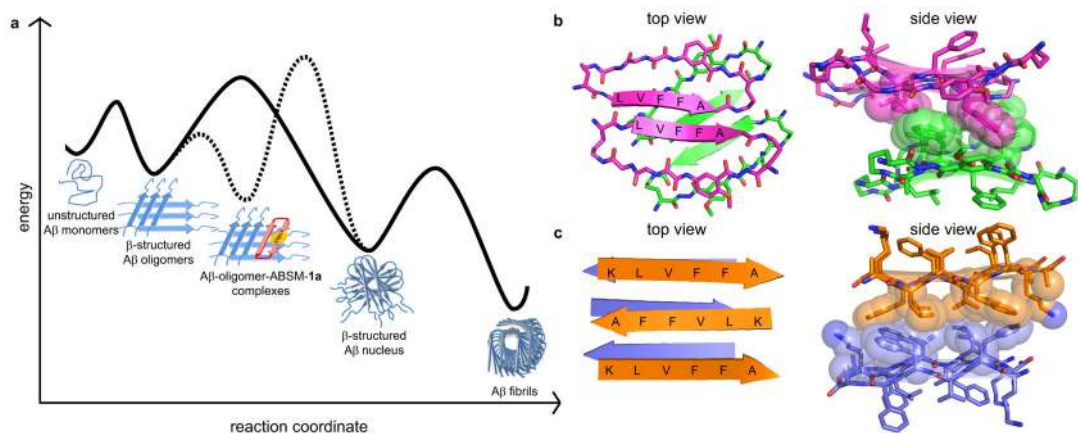
Figure 5.
β-Sheet interactions of Aβ peptides and ABSM **1a**. (a) Proposed model of inhibition of Aβ aggregation by ABSM **1a**. The solid curve corresponds to a pathway in which Aβ aggregates without ABSM **1a**. The dashed curve corresponds to an alternative pathway in which ABSM **1a** inhibits Aβ aggregation by binding Aβ oligomers. (b) Crystal structure of a macrocyclic peptide containing pentapeptide sequence LVFFA[17]. (PDB ID: 3Q9H) The magenta and green structures correspond to parallel and antiparallel β-sheet dimers formed by the macrocyclic peptide. The side view shows hydrophobic contacts formed between the parallel and antiparallel β-sheet dimers. (c) Crystal structure of the linear peptide KLVFFA[35]. (PDB ID: 3OW9) The orange and purple structures correspond to different layers within the crystal structure. The side view shows hydrophobic contacts between the layers.

Table 1
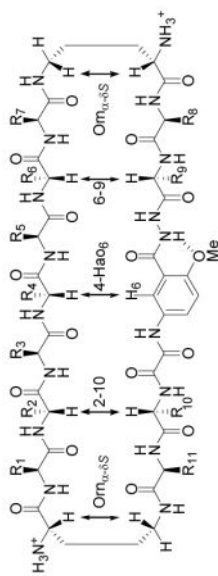
Amino Acid Sequences and Key NOEs of ABSMs 1a–q.

	Sequence	R_1–R_7	R_8–R_{11}	Orn$_{\alpha\text{-}\delta S}$	2–10	4-Hao$_6$	6–9	Orn$_{\alpha\text{-}\delta S}$	Folding
1a	Aβ_{16-22}	KLVFFAE	KLIE	S^a	_^{b}	S	S	S	good
1b	Aβ_{17-23}	LVFFAED	KLIE	S	S	S	S	S	good
1c	Aβ_{29-35}	GAIIGLM	KFYK	S	S	S	S	S	good
1d	Aβ_{30-36}	AIIGLMV	KFYK	S	S	S	S	S	good
1e	Aβ_{30-36} G33F	AIIFLMV	KFYK	S	S	S	S	S	good
1f	Aβ_{34-40}	LMVGGVV	KFYK	S	S	W^a	_^{c}	S	moderate
1g	Aβ_{34-40} G37F	LMVFGVV	KFYK	S	S	S	S	S	good
1h	Sup35$_{7-13}$	GQQNNQY	KFYK	W	_^{c}	_^{c}	_^{c}	W	poor
1i	hPrP$_{116-122}$	AAAGAVV	KFYK	W	W	_^{c}	_^{c}	W	poor
1j	Tau$_{305-311}$	SVQIVYK	EFYK	S	S	S	S	S	good
1k	hβ_2M$_{62-68}$	FYLLYYT	KNSA	S	S	S	_^{b}	S	good
1l	hβ_2M$_{63-69}$	YLLYYTE	FKVS	W	_^{c}	_^{c}	_^{c}	W	poor
1m	hβ_2M$_{63-69}$	YLLYYTE	KVVK	S	_^{d}	S	_^{d}	S	good
1n	hαSyn$_{69-75}$	AVVTGVT	KFYV	S	S	S	_^{d}	S	good
1o	hαSyn$_{75-81}$	TAVANKT	VFYK	S	S	S	_^{d}	S	good
1p	hIAPP$_{11-17}$	RLANFLV	KFYK	S	S	S	S	S	good
1q	hIAPP$_{26-32}$	ILSSTNV	KFYK	S	S	S	S	S	good
1r	Aβ_{30-36}	AIIGLMV	KFF^{Br}K						

[a] S: strong NOE; W: weak NOE.

[b] NOE not observed due to overlap of proton resonances.

[c] NOE not observed.

[d] NOE not able to be observed due to overlap with HOD.